IOP Conf. Series: Journal of Physics: Conf. Series **843** (2017) 012003 doi:10.1088/1742-6596/843/1/012003

eXtended Finite Element Method applied to the strength prediction of adhesively-bonded joints

J.T.S. Xará[a], R.D.S.G. Campilho[a,b,*]

[a] Departamento de Engenharia Mecânica, Instituto Superior de Engenharia do Porto, Instituto Politécnico do Porto, Rua Dr. António Bernardino de Almeida, 431, 4200-072 Porto, Portugal
[b] INEGI – Pólo FEUP, Rua Dr. Roberto Frias, s/n, 4200-465 Porto, Portugal
* raulcampilho@gmail.com

Abstract. High-strength composites are widely used in several industries, such as aeronautical, automotive and naval, and they can be combined with metals to provide significant advantages in structural design. The application of adhesive bonding to these assemblies supposes the existence of reliable design tools to accurately analyse the joints' behaviour. In this context, the eXtended Finite Element Method (XFEM) is a recent possibility to predict bonded' joints fracture behaviour. This work aims to study by XFEM single-*L* adhesive joints between aluminium components and carbon-epoxy composites under peeling loads, considering the variation of the *L*-shaped adherend's thickness (t_{P2}) and adhesives of distinct ductility. The XFEM analysis was either based on stress or strain criteria for assessment of damage initiation, and different damage law types for crack propagation. Validation was undertaken with experimental data. The XFEM analysis revealed that this method is very accurate when using the stress-based quadratic initiation criterion and the triangular propagation law. It was shown that the *L*-shaped adherend's geometry and the adhesive type are the most important parameters affecting the joints' strength.

1. Introduction
Structural bonding using adhesives has been increasing in recent years because of the advantages that this joining method presents over more traditional joining methods such as fastening, welding and riveting. The aeronautical industry is the one that most contributed to the use and development of adhesives. Structural components can be bonded using various types of adhesive joints: single and double-lap joints, scarf joints or single-*L* joints. The single-lap joint is the most common and studied due to its easy fabrication and because the adhesive is mainly loaded with shear (τ_{xy}) stresses [1]. However, this type of joint performs poorly in comparison with other joint configurations due to the eccentric transmission of load resulting in high normal (σ_y) peak stresses at the overlap edges. The double-lap joint solves this problem due to its symmetric configuration [2, 3]. Thus, it is possible to obtain a joint more than twice as strong as a single-lap joint for the same overlap length (L_O) [4]. The use of scarf joints promotes the reduction of peak stresses in the adhesive layer, which results in a higher strength per bonded area. Single-*L* joints have some similarities with *T*-joints but, instead of having only two *L*-shaped adherends facing each other and bonded to a flat adherend, only one *L*-part is considered. Li et al. [5] studied the stress distributions in the adhesive layer of a single-*L* joint using a Finite Element Method (FEM) analysis. The joint was analysed under three loading conditions, two linear loads and one bending moment (*M*). The results allowed to conclude that the loading in the *y*-direction (P_y) is the

most harmful to the adhesive layer by resulting in higher peak stresses in comparison with the loading in the *x*-direction (P_x) and *M*. It was also shown in a parametric study on L_O that, as this parameter increased, the peak peel stresses gradually diminished.

Failure prediction in adhesive joints can be undertaken using two alternatives: analytical and numerical methods. Analytical methods consist of closed-form analyses. Numerical methods, such as the FEM, are more suitable to model joints with complex geometries and elaborate material models. Continuum mechanics modelling by FEM is based on a stress or strain limit state and give good results provided that the failure criteria are properly selected. Damage mechanics modelling, based either on stress intensity factors or energetic approaches, induce damage in the models by the onset and propagation of cracks. This method allows the possibility to simulate fracture and step-by-step damage at a pre-defined crack path or arbitrarily with a finite region up to complete structural failure. Cohesive Zone Modelling (CZM) is a damage mechanics-based technique that can be incorporated in FEM analyses to promote static or fatigue damage in structures. The XFEM is an improvement of the FEM standard modelling procedure to induce damage growth. XFEM damage modelling excels CZM by enabling cracks to grow freely through continuum-based finite elements without the requirement of introducing special purpose elements. Campilho et al. [6] evaluated the CZM and XFEM techniques for the strength prediction of single and double-lap bonded joints with aluminium adherends and a brittle adhesive (Araldite® AV138). The CZM results were accurate but damage growth in the adhesive could not be simulated by the XFEM because of the mode-mixity. Mubashar et al. [7] studied adhesive joints by combining CZM and XFEM. The XFEM was used for crack modelling in the adhesive fillets and bond length, and the CZM was used for the interfaces between the fillet/adhesive bond and the adherends. It was concluded that the XFEM could predict the crack trajectory in the adhesive region of an adhesive joint. This hybrid model proved to be efficient in predicting the crack initiation and growth and also in estimating the strength of adhesive joints. Curiel Sosa and Karapurath [8] studied the application of the XFEM in modelling delamination damage in Fibre Metal Laminates (FML) under mode I loading by the Double-Cantilever Beam (DCB) configuration. In order to validate the XFEM analysis, the load-displacement (P-δ) curves were compared with the experimental results and with a CZM simulation from another work (Airoldi et al. [9]), and a good match was found.

This work aims to study by XFEM single-*L* adhesive joints between aluminium components and carbon-epoxy composites under peeling loads, considering the variation of t_{P2} and adhesives of distinct ductility. The XFEM analysis was either based on stress or strain criteria for assessment of damage initiation, and different damage law types for crack propagation. Validation was undertaken with experimental data and also CZM results from a previous work [10].

2. Experimental work

The experimental work considered a carbon-fibre reinforced plastic (CFRP) pre-preg (SEAL® Texipreg HS 160 RM) with a ply thickness of 0.15 mm for the flat adherends of the single-*L* joint, to produce a unidirectional laminate ($[0]_{20}$). The fabrication of the composite adherends consisted of manually stacking 20 layers of CFRP and curing for 1 hour at 130 ºC and pressure of 2 bar in a hot plates press. Table 1 presents the elastic orthotropic properties of a unidirectional carbon-epoxy ply aligned in the fibres direction to be used in the numerical simulations [10].

Table 1 – Elastic orthotropic properties of a unidirectional carbon-epoxy ply aligned in the fibres direction (*x*-direction; *y* and *z* are the transverse and through-thickness directions, respectively) [10].

E_x=1.09E+05 MPa	ν_{xy}=0.342	G_{xy}=4315 MPa
E_y=8819 MPa	ν_{xz}=0.342	G_{xz}=4315 MPa
E_z=8819 MPa	ν_{yz}=0.380	G_{yz}=3200 MPa

The *L*-shaped adherends are made of a high-strength aluminium alloy sheet (AA6082 T651), whose relevant mechanical properties are as follows: Young's modulus (*E*) of 70.1±0.8 GPa, tensile yield stress

(σ_e) of 261.7±7.7 MPa, tensile failure strength (σ_f) of 324.0±0.2 MPa and tensile failure strain (ε_f) of 21.7±4.2%.

The adhesives considered in the experimental work are the following: the Araldite® AV138, a brittle epoxy, and the SikaForce® 7752, a highly ductile polyurethane. The relevant properties to be obtained for the adhesives are E, the shear modulus (G), the strengths in tension (t_n^0) and shear (t_s^0), G_{IC} and the shear fracture toughness (G_{IIC}). Table 2 presents all data obtained for the two adhesives used in this work.

Table 2 – Properties of the adhesives Araldite® AV138 and Sikaforce® 7752 [6, 11, 12].

Property	**AV138**	**7752**
Young's modulus, E [GPa]	4.89±0.81	0.49±0.09
Poisson's ratio, ν	0.35 *	0.30 [a]
Tensile yield strength, σ_y [MPa]	36.49±2.47	3.24±0.48
Tensile failure strength, σ_f [MPa]	39.45±3.18	11.48±0.25
Tensile failure strain, ε_f [%]	1.21±0.10	19.18±1.40
Shear modulus, G [GPa]	1.56±0.01	0.19±0.01
Shear yield strength, τ_y [MPa]	25.1±0.33	5.16±1.14
Shear failure strength, τ_f [MPa]	30.2±0.40	10.17±0.64
Shear failure strain, γ_f [%]	7.8±0.7	54.82±6.38
Toughness in tension, G_{IC} [N/mm]	0.20 [a]	2.36±0.17
Toughness in shear, G_{IIC} [N/mm]	0.38 [a]	5.41±0.47

* manufacturer's data

[a] estimated in reference [6], [b] estimated from Hooke's law

The geometry and respective dimensions of the single-*L* joints are represented in Fig. 1. The dimensions considered are (in mm): L_O=25, out-of-plane width of the joint b=25, specimen length L_T=80, flat adherend thickness t_{P1}=3, t_{P2}=1, 2, 3 and 4, curved element free length L_A=60, curved element radius R=5 and t_A=0.2.

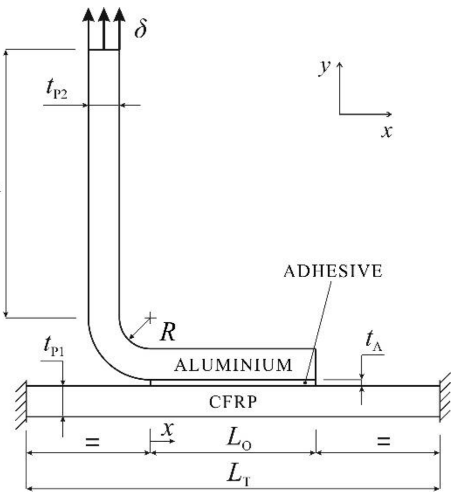

Fig. 1 – Geometry and dimensions of the single-*L* joint.

The fabrication of the single-*L* joints consisted of several steps. First, CFRP plates were manufactured using an unidirectional CFRP pre-preg in order to produce the base adherends of the joint. The fabrication of the composite plates was performed by manual stacking followed by curing in a hot plates press under specified pressure and heat conditions. Bending of the aluminium adherends was executed using a manual bending machine after cutting to the final dimensions from a laminated aluminium plate. Surface preparation of both aluminium and CFRP adherends consisted of manual abrasion with fine mesh sandpaper and cleaning with acetone. After, the adherends were bonded using a steel mould in order to guarantee a correct alignment and using calibrated spacers to ensure the stipulated t_A value. The adhesive layer curing lasted for one week and the removal of the excess adhesive at the specimens' side was performed by precision milling. The tensile tests were executed in an Instron® 3367, which is an electro-mechanical testing machine, with a 30 kN load cell. These tests were carried out at room temperature and constant velocity of 0.5 mm/min. Five specimens were tested for each joint configuration.

3. Numerical work

The geometrically non-linear and two-dimensional XFEM analysis was undertaken in the FEM software Abaqus®. Both the adherends and adhesive were regarded as elasto-plastic with solid FEM elements (plane-strain elements with the Abaqus® reference CPE4) Apart from this, an enriched XFEM formulation was considered for the adhesive layer's solid elements. Fig. 2 gives an example of mesh refinement for the XFEM simulations.

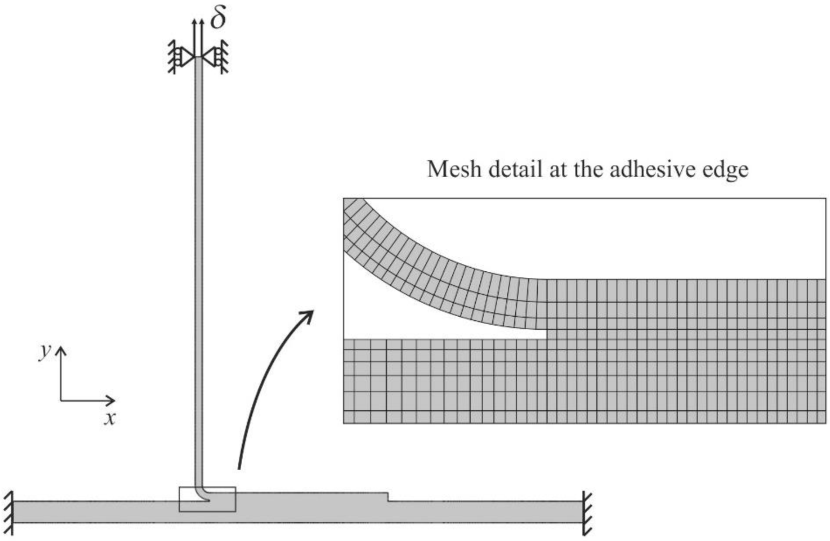

Fig. 2 – Boundary conditions and mesh detail at the adhesive edge (example for joint with t_{P2}=1 mm).

Table 3 – Parameters of the Araldite® AV138 and SikaForce® 7752 for XFEM modelling.

Property	**AV138**	**7752**
E [GPa]	4.89	0.49
G [GPa]	1.56	0.19
σ_{max}^0 [MPa]	39.45	11.48
ε_{max}^0 [%]	1.21	19.18
t_n^0 [MPa]	39.45	11.48
t_s^0 [MPa]	30.2	10.17
ε_n^0 [%]	1.21	19.18
ε_s^0 [%]	7.8	54.82

All meshes were constructed taking advantage of bias effects to increase the computational efficiency. The finite element's size was graded across L_O to provide a higher refinement near the overlap edges, vertically in the adherends towards the adhesive layer, and also in the unbonded portion of the adherends in the direction of the bond. The quadrilateral elements' size in the adhesive layer was defined as 0.2×0.2 mm^2. To be consistent with the experimental tests, the boundary conditions consisted of clamping the base CFRP adherend at both sides, and horizontal restraining and tensile loading the upper edge of the *L*-part (Fig. 2). Table 3 summarizes the parameters introduced in Abaqus® for XFEM modelling, obtained from the data of Table 2. For a full description of the XFEM formulation, the reader can refer to the Abaqus® documentation [13].

4. Results

4.1. Experimental strength

Fig. 3 shows the experimental maximum load (P_m) values for the joints with the Araldite® AV138 and Sikaforce® 7752 as a function of t_{P2}.

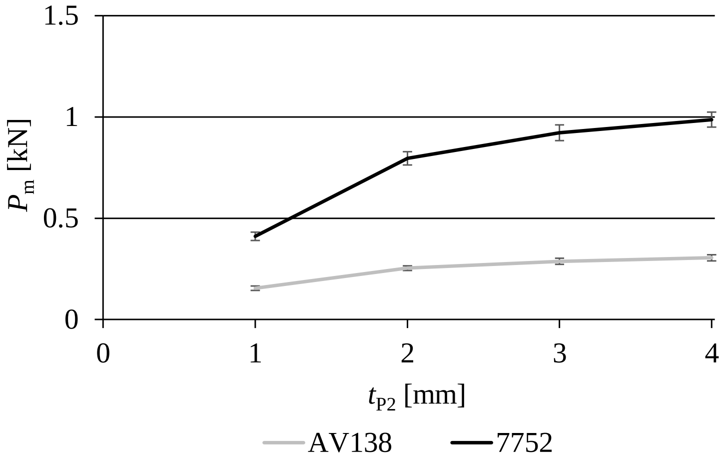

Fig. 3 – Experimental P_m values for the joints with the Araldite® AV138 and Sikaforce® 7752.

The joints with the Araldite® AV138 revealed a major P_m increase between t_{P2}=1 and 2 mm (64.5%), but this improvement gradually diminishes for higher t_{P2} (compared to t_{P2}=1 mm, improvement of 86.3% for t_{P2}=3 mm and 97.5% for t_{P2}=4 mm). The P_m improvement was found to be related to the increased stiffness of the *L*-part, which in turn reduced σ_y peak peel stresses and enabled spreading σ_y stresses across a larger length in the adhesive. Compared to these joints, for the joints with the Sikaforce® 7752 P_m is much higher, although this adhesive is less strong (Table 2). It was found that, depending on t_{P2}, P_m for this adhesive can exceed 3 times P_m of the Araldite® AV138, even though the Sikaforce® 7752 has practically ¼ of the tensile strength. However, the Sikaforce® 7752 is much less stiff (Table 2), leading to flatter σ_y stress plots in the vicinity of the damage initiation site (pull-out edge of the adhesive layer). For this adhesive, the P_m increase from the joint configuration with t_{P2}=1 mm is 93.5% (t_{P2}=2 mm), 124.3% (t_{P2}=3 mm) and 140.1% (t_{P2}=4 mm). Compared to the Araldite® AV138, the evolution of P_m with t_{P2} is higher, because of the increased capacity of the adhesive to plasticize further within the adhesive layer.

4.2. Strength prediction

4.2.1. Study of the damage initiation criterion. A triangular growth law was used in all simulations of this Section. The linear energetic propagation criterion was used. Fig. 4 gives two examples of crack growth in the adhesive layer for the MAXS (maximum nominal stress), MAXE (maximum nominal strain), QUADS (quadratic nominal stress) and QUADE (quadratic nominal strain) criteria (a) and MAXPS (maximum principal stress) and MAXPE (maximum principal strain) criteria (b), in both cases considering a joint with t_{P2}=1 mm.

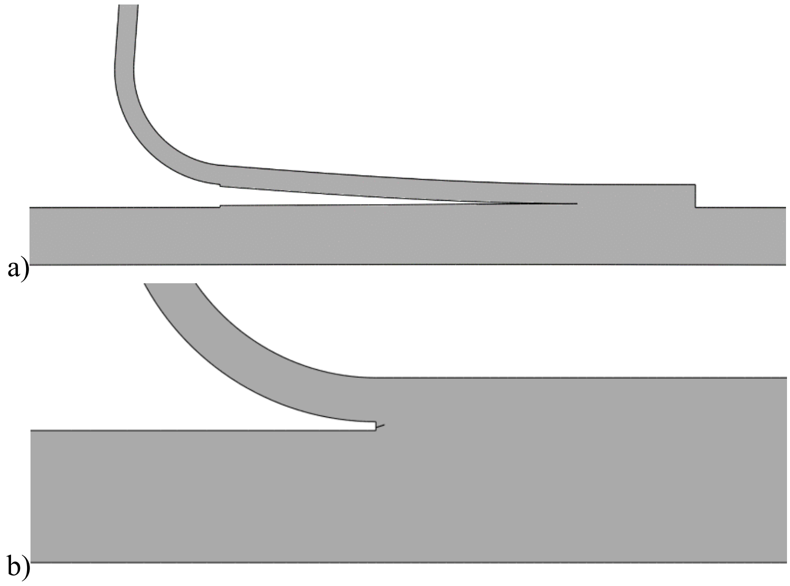

Fig. 4 – Example of crack growth in the adhesive layer for the MAXS, MAXE, QUADS and QUADE criteria (a) and MAXPS and MAXPE criteria (b).

Fig. 5 shows a comparison between the experimentally obtained P_m values and the respective numerical predictions of the different XFEM damage initiation criteria, for the two tested adhesives and as a function of t_{P2}.

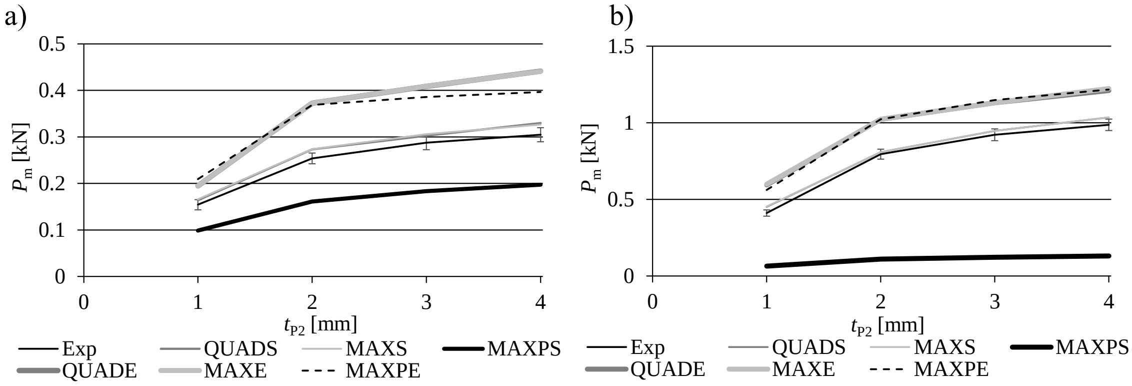

Fig. 5 – Experimental and numerical P_m values with different damage initiation criteria for the joints with the Araldite® AV138 (a) and Sikaforce® 7752 (b).

For the Araldite® AV138 (Fig. 5 a), by comparison with the experiments, the QUADS and MAXS criteria clearly provide the best P_m predictions. Nonetheless, for most t_{P2} values the numerical P_m points are slightly above the experimental range defined by the respective scatter. Compared to the experimentally obtained values, for the QUADS criterion and the four values of t_{P2} (1, 2, 3 and 4 mm), the percentile variations are 6.9%, 7.7%, 5.4% and 8.2%, respectively. Considering the MAXS criterion, the percentile variations are 7.5%, 7.8%, 6.4% and 7.2%, by the same order. The other stress-based criterion, MAXPS, has proved not to work well in the technique that it was applied, giving a maximum percentile variation to the experiments of -59.9%. The strain-based criteria (QUADE, MAXE and MAXPE) all overestimated the values of P_m. The maximum percentile deviations were 46.8%, 46.8% and 45.3% for the QUADE, MAXE and MAXPE criteria, respectively (in all cases for t_{P2}=2 mm). The accuracy of the predictions by applying the same six damage initiation criteria for the joints bonded with the SikaForce® 7752 (Fig. 5 b) is qualitatively identical to those obtained with the Araldite® AV138, although P_m have a different magnitude. The QUADS and MAXS damage initiation criteria were again the most accurate and, for this adhesive, the numerical values were mostly within the experimental range. In the case of the QUADS criterion, the percentile variation to the average experimental values was 9.7%, 1.6%, 2.7% and 4.8% for increasing t_{P2} between 1 and 4 mm. For the MAXS criterion, the same deviation was 10.1%, 1.6%, 2.7% and 4.8%, for t_{P2}=1, 2, 3 and 4 mm, respectively. These two criteria behave similarly, resulting in similar % differences. The MAXPS results revealed the highest offset to the experimental data, presenting a maximum percentile deviation of -86.8%. The predictions with the three initiation criteria based on strains (QUADE, MAXE and MAXPE) presented relatively approximate values among them but significantly offset to the experimental P_m values. Based on the experimental results, the maximum percentile deviations were 44.6%, 45.9 and 36.6% for the QUADE, MAXE and MAXPE criteria, respectively (in all cases for t_{P2}=1 mm).

4.2.2. Study of the law shape and damage growth criterion. As a complement of the former analysis on the damage initiation criterion, a comparison was also carried out regarding the softening law shape during damage growth. The triangular law results obtained in the previous analysis are thus compared with numerical predictions using an exponential law and power law exponents of 0.5, 1 and 2. All numerical simulations considered the QUADS damage initiation criterion. Fig. 6 compares P_m regarding these conditions and the experimental data for the joints bonded with the adhesives Araldite® AV138 (a) and SikaForce® 7752 (b).

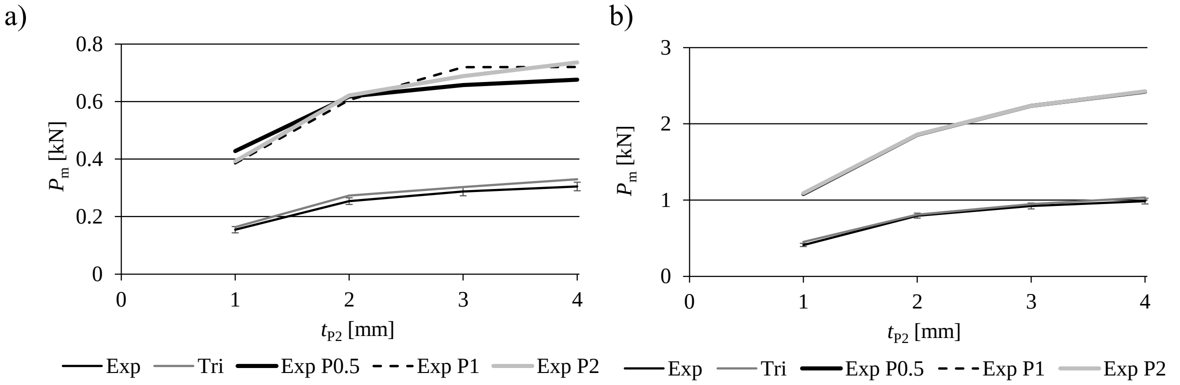

Fig. 6 – Experimental and numerical P_m values with different law shapes and damage growth criteria for the joints with the Araldite® AV138 (a) and Sikaforce® 7752 (b).

For the joints bonded with the Araldite® AV138, the exponential propagation law greatly overestimates P_m, for the three tested values of α. A maximum percentile different to the average experimental values of 160.9%, 137.6% and 139.4% was attained for α=0.5, 1 and 2, respectively. Identically, for the joints bonded with the Sikaforce® 7752, the exponential propagation law resulted in a large deviation of P_m compared to the experiments. A maximum percentile variation between the simulations with an exponential law and the experimental tests of 139.5%, 139.5% and 141.9% was found for α=0.5, 1 and 2, respectively. For both adhesives, this large difference is justified by the higher failure displacements resulting from the exponential damage laws, which artificially enlarge the damage length in the adhesive.

5. Conclusions

This work aimed at studying the behaviour of hybrid single-*L* bonded joints between aluminium and CFRP adherends, considering different geometric conditions (t_{P2} values) and adhesives of different strength and ductility. The experimental analysis showed that the Sikaforce® 7752 adhesive gives the best results in this particular joint configuration for all t_{P2} values tested, showing that a less strong but ductile adhesive behaves better in this joint configuration than a stronger but more brittle adhesive. The percentile P_m improvement for the joints bonded with the Sikaforce® 7752 over those bonded with the Araldite® AV138 was 166.3%, 213.4%, 220.7% and 223.9% for increasing t_{P2} between 1 and 4 mm.

IOP Conf. Series: Journal of Physics: Conf. Series **843** (2017) 012003 doi:10.1088/1742-6596/843/1/012003

The geometric parameter t_{P2} largely influences the joints' strength, with advantage of higher values. A detailed study was then undertaken to validate the XFEM technique for strength prediction of these joints. The study of the effect of the damage initiation criterion showed that the QUADS and MAXS criteria give the most accurate results. Considering the joints bonded with the Araldite® AV138, for the QUADS criterion the maximum error compared to the average experimental values was 8.2% (t_{P2}=4 mm),while for the MAXS criterion it was 7.8% (t_{P2}=2 mm). The maximum errors for the joints bonded with the Sikaforce® 7752 were 9.7% (t_{P2}=1 mm) for the QUADS criterion and 10.1% (t_{P2}=1 mm) for the MAXS criterion. The strain-based criteria (QUADE, MAXE and MAXPE) largely overestimated P_m for both adhesives. For both adhesives, the MAXPS criterion proved to be the most misfit criterion. The study of the propagation law showed that the triangular law is much more accurate than the exponential law, which is not considered suitable to model the behaviour of adhesive joints. It is thus concluded that the XFEM, using the aforementioned criterion and growth law, is a very precise tool for the strength prediction of single-*L* joints bonded with adhesives ranging from brittle to ductile.

References

[1] R.D.F. Moreira, R.D.S.G. Campilho, Parametric Study of the Reinforcement Geometry on Tensile Loaded Scarf Adhesive Repairs, J. Adhesion 92(7-9) (2016) 586-609.
[2] S.L.S. Nunes, R.D.S.G. Campilho, F.J.G. da Silva, C.C.R.G. de Sousa, T.A.B. Fernandes, M.D. Banea, L.F.M. da Silva, Comparative failure assessment of single and double-lap joints with varying adhesive systems, J. Adhesion 92 (2016) 610-634.
[3] U.T.F. Carvalho, R.D.S.G. Campilho, Application of the direct method for cohesive law estimation applied to the strength prediction of double-lap joints, Theor. Appl. Fract. Mec. 85, Part A (2016) 140-148.
[4] K.C. Shin, J.J. Lee, Bond Parameters to Improve Tensile Load Bearing Capacities of Co-Cured Single and Double Lap Joints with Steel and Carbon Fiber-epoxy Composite Adherends, J. Compos. Mater. 37(5) (2003) 401-420.
[5] W. Li, L. Blunt, K.J. Stout, Analysis and design of adhesive-bonded tee joints, Int. J. Adhes. Adhes. 17(4) (1997) 303-311.
[6] R.D.S.G. Campilho, M.D. Banea, A.M.G. Pinto, L.F.M. da Silva, A.M.P. de Jesus, Strength prediction of single- and double-lap joints by standard and extended finite element modelling, Int. J. Adhes. Adhes. 31(5) (2011) 363-372.
[7] A. Mubashar, I.A. Ashcroft, A.D. Crocombe, Modelling damage and failure in adhesive joints using a combined XFEM-cohesive element methodology, J. Adhesion 90(8) (2014) 682-697.
[8] J.L. Curiel Sosa, N. Karapurath, Delamination modelling of GLARE using the extended finite element method, Composites Science and Technology 72(7) (2012) 788-791.
[9] A. Airoldi, M. Vesco, S. van der Zwaag, A. Baldi, G. Sala, Damage in GLARE laminates under indentation loads: experimental and numerical results, Proceedings of the 17th international conference on composite materials, Edinburgh, UK, 2009.
[10] N.R.E. Domingues, R.D.S.G. Campilho, R.J.C. Carbas, L.F.M. da Silva, Experimental and numerical failure analysis of aluminium/composite single-L joints, Int. J. Adhes. Adhes. 64 (2016) 86-96.
[11] R.D.S.G. Campilho, M.D. Banea, J.A.B.P. Neto, L.F.M. da Silva, Modelling adhesive joints with cohesive zone models: effect of the cohesive law shape of the adhesive layer, Int. J. Adhes. Adhes. 44 (2013) 48-56.
[12] T. Faneco, R. Campilho, F. Silva, R. Lopes, Strength and Fracture Characterization of a Novel Polyurethane Adhesive for the Automotive Industry, J. Test. Eval. 45(2) (2017) n.a.
[13] Abaqus®, Documentation, in: D. Systèmes (Ed.) Vélizy-Villacoublay, 2013.